54

Hadron spectroscopy

54.1 Light $\bar{q}q$ mesons

The spectroscopy of the light mesons has been discussed extensively in the literature, using LSR [1,357,3,32,452], FESR [405,629], and Yndurain's moments within positivity [730]. Detailed derivations of the analysis in some channels can e.g. be found in QSSR1 [3]. In addition to the currents associated to the (axial)-vector and (pseudo)scalar channels, discussed in previous chapters, we shall also be concerned with the 2^{++} tensor current, where its renormalization has been discussed in Part VIII, while the corresponding sum rule has been re-analysed in [452]. The analysis is summarized in Table 54.1, where one can deduce from Table 54.1, that the predictions for the couplings are quite good compared with available data, whereas in some cases the meson masses are overestimated.

54.2 Light baryons

As mentioned earlier, the light baryon systems have been studied in [424–430]. The decuplet and the octet baryons can be respectively described by the operators:

$$\Delta^{\mu} = \frac{1}{\sqrt{2}} \; : \; \psi^T C \gamma_{\lambda} \psi \left(g^{\mu\lambda} - \frac{\gamma^{\mu}\gamma^{\lambda}}{4} \right) \psi \; , \tag{54.1}$$

and:

$$N = \frac{1}{\sqrt{2}} : [\, (\psi C \lambda_5 \psi)\, \psi + b\, (\psi C \psi)\, \lambda_5 \psi \,] \; , \tag{54.2}$$

where C is the charge conjugation matrix, b is an arbitrary mixing parameter and ψ is the *valence* quark field. We have suppressed the colour indices. The corresponding two-point correlator:

$$S(q) = i \int d^4x \; e^{iqx} \langle \, 0 | \mathcal{T} \mathcal{O}(x) \mathcal{O}^{\dagger}(0) | 0 \, \rangle \; , \tag{54.3}$$

can be parametrized (without loss of generalities) in terms of two invariants:

$$S(q) = (\hat{q} F_1 + F_2)\, \Gamma + \cdots \; , \tag{54.4}$$

where for the decuplet ($\Delta(3/2)$) $\Gamma \equiv g^{\mu\nu}$, and for the octet (nucleon) $\Gamma = 1$. The expressions of the form factors are known including radiative corrections and non-perturbative

https://doi.org/10.1017/9781009290296.068 Published online by Cambridge University Press

Table 54.1. *Light meson masses and couplings from QSSR. The coupling f_P are in units of MeV and normalized as $f_\pi = 92.4$ MeV, while γ_V has no dimension and is normalized as $\gamma_\rho = 2.55$ (Eq. 2.52). WSR refer to Weinberg sum rules in QCD (previous chapter)*

J^{PC}	Meson	Coupling	Mass (GeV)	t_c (GeV^2)	τ (GeV^{-2})	References
1^{--}	ρ	$\gamma_\rho \simeq 2.5 \sim 2.8$	$0.80 \sim 0.85$	$1.4 \sim 1.7$	$0.4 \sim 1$	[3]
	K^*	$\gamma_{K^*} \simeq 2.0 \sim 2.5$		$1.4 \sim 2$	$0.6 \sim 1$	[3]
1^{++}	A_1	$\gamma_{A_1} \simeq (1.2 \sim 1.9)\gamma_\rho$	1.28	$2.0 \sim 2.3$	$0.6 \sim 1$	WSR [29,3]
0^{-+}	π	$f_\pi \simeq (74 \sim 96)$	$\pi^+ - \pi^0 \simeq 4.6 \times 10^{-3}$	$1.8 \sim 2.3$	$0.7 \sim 1.6$	[30,29,3]
	K'	$\frac{M_{K'}^4 f_{K'}^2}{M_K^4 f_K^2} \simeq 9.5 \pm 2.5$		$1.8 \sim 2.3$	$0.7 \sim 1.6$	[3]
0^{++}	$a_0(\bar{u}d)$	$f_a \simeq (1.6 \pm 0.5)$	$1.0 \sim 1.05$	$1.3 \sim 1.6$	$0.4 \sim 0.8$	[3,420,422]
	$f_0(\bar{u}u + \bar{d}d)$	$f_{f_0} \simeq f_a$	$M_{f_0} \simeq M_{a_0}$			$SU(2)$
	$K_0^*(\bar{u}s)$	$f_{K_0^*} \simeq (46.3 \pm 7.5)$	$1.3 \sim 1.4$	$1.8 \sim 2.3$	$0.7 \sim 1.6$	[419,3,420,422]
	$f_0(\bar{s}s)$	$f_3 \simeq (22 \sim 28)$	1.474 ± 0.044	$\simeq t_c^{K^*0}$	$0.3 \sim 0.5$	[688,3]
2^{++}	f_2	$f_{f_2} \simeq (132 \sim 184)$	$1.4 \sim 1.6$	$2.5 \sim 3.5$	$0.6 \sim 1.2$	[452,3]
	f_2'	$f_{f_2'} \simeq (112 \sim 152)$	$\frac{M_{f_2'}}{M_{f_2}} \simeq 1.14 \sim 1.26$	$3 \sim 4$	$0.6 \sim 1.2$	[452,3]

terms. These terms are tabulated in [426] (see chapter on two-point function). The relevant quantities for the analysis are the LSR:

$$\mathcal{L}_i(\tau) = \int_0^{t_c} dt\ e^{-t\tau} \frac{1}{\pi} \text{Im} F_i(t)\ :\quad i = 1, 2 \tag{54.5}$$

and their ratios:

$$R_{ii}(\tau) = \frac{\int_0^{t_c} dt\ t\ e^{-t\tau} \frac{1}{\pi} \text{Im} F_i(t)}{\int_0^{t_c} dt\ e^{-t\tau} \frac{1}{\pi} \text{Im} F_i(t)}\ , \tag{54.6}$$

and:

$$R_{12}(\tau) = \frac{\int_0^{t_c} dt\ e^{-t\tau} \frac{1}{\pi} \text{Im} F_2(t)}{\int_0^{t_c} dt\ e^{-t\tau} \frac{1}{\pi} \text{Im} F_1(t)}\ . \tag{54.7}$$

The baryon contribution to the spectral function can be introduced through its coupling and using a duality ansatz parametrization:

$$\begin{aligned} \frac{1}{\pi} \text{Im} F_2(t) &= M_B |Z_B|^2 \delta\left(t - M_B^2\right) + \Theta(t - t_c)\ \text{`QCD continuum'}\ , \\ \frac{1}{\pi} \text{Im} F_1(t) &= |Z_B|^2 \delta\left(t - M_B^2\right) + \Theta(t - t_c)\ \text{`QCD continuum'}\ . \end{aligned} \tag{54.8}$$

Qualitatively, $\mathcal{R}_{12}$ can provide a good explanation of the proton mass in terms of the chiral condensate:

$$M_N \approx 32\pi^2 \langle \bar{\psi}\psi \rangle \tau \left(\frac{7 - 2b - 5b^2}{5 + 2b + 5b^2} \right)\ . \tag{54.9}$$

https://doi.org/10.1017/9781009290296.068 Published online by Cambridge University Press

Table 54.2. *Light baryon masses and couplings from QSSR*

Baryon	Coupling (GeV^6)	Mass (GeV)	Mass (GeV) (exp)	t_c (GeV^2)
Octet:	$J^P = (1/2)^+$			
N	0.14	1.05	0.94	1.58
Σ	0.27	1.16	1.19	2.09
Λ	0.23	1.24	1.1	2.15
Ξ	0.31	1.33	1.31	2.42
Decuplet:	$J^P = (3/2)^+$			
Δ	1.15	1.21	1.23	2.2
Ω	5.16	1.61	1.67	4.08
Σ^*	1.89	1.35	1.38	2.78
Ξ^*	3.07	1.48	1.51	3.39

One can optimize this relation in the change of the mixing parameter b by requiring that its first derivative in b is zero (Principle of Minimal Sensitivity), which gives:

$$b = -\frac{1}{5}\,, \tag{54.10}$$

which is the optimal choice of Chung *et al.* [424] obtained after an involved numerical analysis. The value of the sum rule at which the sum rule is optimized is approximately $\tau^{-2} \approx M_N^2$, from which one can deduce the interesting sum rule:

$$M_N \approx \left[-\pi^2 \frac{152}{3}\langle\bar{\psi}\psi\rangle\right]^{1/3} \approx 1.8 \text{ GeV}\,, \tag{54.11}$$

which is not too bad taking into account the crude approximation used to get this formula. However, it shows the rôle of the non-leading terms in correctly fixing the mass of the nucleon. A comparison of the numerical ability of these different sum rules has been discussed in [2], where it has been noted that $\mathcal{L}_2$ and $\mathcal{R}_{22}$ are the most advantageous sum rule (stability, small radiative correction, ...). The results from this analysis are given in [426] and discussed in details in [3]. We show them in Table 54.2.

We have only quoted in Table 54.2 the central value, where the error is typically about 10%. The different sum rules optimize for τ around $0.8 \sim 1.2$ GeV^{-2}, while the t_c values quoted in the table come from the lowest FESR moment. The results for the octet corresponds to the optimal value $b = -1/5$ discussed earlier. A compromise value:

$$M_0^2 \simeq 0.8 \text{ GeV}^2\,, \tag{54.12}$$

of the scale parametrizing the mixed condensate is needed, as also required for fitting the heavy-light B and B^* meson masses [401]. The $SU(3)$ mass-splittings need large flavour breakings of the chiral condensates $\langle\bar{s}s\rangle$ and $\langle\bar{s}Gs\rangle$, which, at the order we are working to, seem to act in opposite directions. In particular, the Ω mass can be reproduced for a 40% increase of the mixed condensate value compared with its $SU(3)$ symmetric value.

https://doi.org/10.1017/9781009290296.068 Published online by Cambridge University Press

54.3 Spectroscopy of the heavy-light hadrons

54.3.1 Beautiful mesons

The masses and mass-splittings of heavy-light mesons made with $\bar{q}b$ quarks (q is the light quark u, d and s) have been analysed in [401] using the ratio r_n and double ratios d_n of $q^2 = 0$ moments:

$$d_n \equiv \frac{r_n^H}{r_n^{H'}} \,, \tag{54.13}$$

where r_n has been defined analogously to Eq. (54.6); H and H' are the indices of the corresponding meson. The analysis shows a good $n \simeq 7 \sim 9$ and $t_c \simeq (40 \sim 60)$ GeV^2 stabilities, which indicates that the sum rule can give a much better prediction for the ratio than for the absolute values of the meson masses. The observed masses of the B and B^* mesons have been used for fixing the b quark mass and the value of the mixed condensate. The predictions for the mass splittings are given in the table of [313] (Section 51.3). The main features of the results are summarized below.

- **Splittings between the chiral partners**
  Typically, the mass splitting between the meson and its chiral partner is [313]:

$$B_\delta(0^{++}) - B(0^{-+}) \approx B_A^*(1^{++}) - B^*(1^{--}) \simeq (417 \pm 212)\ \text{MeV} \,, \tag{54.14}$$

  which is mainly due to the chiral quark condensate as expected from general arguments.
- **Splittings due to $SU(3)$ breakings**
  The $SU(3)$ breaking mass-splitting is given in [313], as function of the ratio of the normal ordered condensate $\chi = \langle \bar{s}s \rangle / \langle \bar{u}u \rangle$. Using the experimental value $B_s = 5.37$ GeV, one can deduce:

$$\chi \approx 0.75 \,, \tag{54.15}$$

  in agreement with the result obtained from the light meson systems discussed previously. The mass of the B_s^* meson is also given in [401] as a function of χ. Using the previous value of χ, into the prediction of the B_s^* in [401] leads to a value slightly higher than the data [16], and needs to be reconsidered.
- **Decay constants and couplings**
  Besides the decay constants $f_{B_{(s)}}$ of the $B_{(s)}$ mesons which plays an important role in the $B^0_{(s)} - \bar{B}^0_{(s)}$ mixing matrix elements, which we shall discuss in more details in the next chapter, we give below the findings of [401] for the couplings and decay constants of the other mesons to order α_s:

$$f_{B_\delta} \simeq (1.99 \pm 0.39) f_\pi \,, \qquad f_{B^*} \equiv \frac{M_{B^*}}{2\gamma_{B^*}} \simeq f_{B_A^*} \simeq (1.78 \pm 0.22) f_\pi \tag{54.16}$$

  compared with the values of f_B and f_{B_s} obtained to the same order in [717,698,716].

54.3.2 Baryons with one heavy quark

The masses and couplings of the baryons (Quu) where $Q \equiv b, c$ have been estimated [453] using $q^2 = 0$ moments and LSR. In the case of charmed baryons, the LSR stabilizes at

https://doi.org/10.1017/9781009290296.068 Published online by Cambridge University Press

$\tau \simeq 0.4\ \text{GeV}^{-2}$ and for t_c in the range 8 to 16 GeV^2, where the first value corresponds to the beginning of τ stability, while the second one to the t_c stability. Moreover, a study of the stability on the change of the mixing parameter b for the Σ_Q currents lead to the range:

$$-0.5 \leq b \leq 0.5\ , \tag{54.17}$$

in favour of the Chung *et al.* [424] choice $b = -1/5$ in the light baryons sector. In the case of beautiful baryons, the optimal results are obtained for $\tau \simeq 0.2\ \text{GeV}^{-2}$ (LSR), $n \simeq 4 \sim 6$ (moments), and for $t_c \simeq 40 \sim 50\ \text{GeV}^2$. The analysis leads, to a good accuracy, to the mass difference [453]:

$$\Sigma_b - \Sigma_c \simeq 3.4\ \text{GeV}\ , \qquad \Sigma_b^* - \Sigma_c^* \simeq 3.3\ \text{GeV}\ . \tag{54.18}$$

Using the experimental value of Σ_c, one can then predict [453]:

$$\Sigma_b \simeq 5.85\ \text{GeV}\ , \tag{54.19}$$

in agreement with the potential model estimate. The corresponding couplings are:

$$|Z_{\Sigma_c}|^2 \simeq (4.2 \sim 7.7) \times 10^{-4}\ \text{GeV}^6\ , \qquad |Z_{\Sigma_b}|^2 \simeq (0.10 \sim 0.45) \times 10^{-2}\ \text{GeV}^6\ , \tag{54.20}$$

where we have used the same normalization as in the light baryon systems. To a lesser accuracy, one has also obtained [453]:

$$\Sigma_c^* \simeq (2.15 \sim 2.92)\ \text{GeV}\ , \qquad \Sigma_b^* \simeq (5.4 \sim 6.2)\ \text{GeV}\ , \tag{54.21}$$

in agreement with potential model estimates. The corresponding couplings are:

$$|Z_{\Sigma_c^*}|^2 \simeq (1.1 \sim 2.2) \times 10^{-3}\ \text{GeV}^6\ , \qquad |Z_{\Sigma_b}|^2 \simeq (2.0 \sim 5.4) \times 10^{-3}\ \text{GeV}^6\ . \tag{54.22}$$

The analysis has been also applied to the Λ_Q baryon. One has obtained [453]:

$$\Sigma_c - \Lambda_c \leq 207\ \text{MeV}\ , \qquad \Sigma_b - \Lambda_b \leq 163\ \text{MeV}\ , \tag{54.23}$$

where the bounds should be understood as 'practical' though not 'rigorous'. One can also notice that the value of the Λ_Q mass decreases with the value of the gluon condensate. Finally, the previous analysis for the baryons has been extended in the case where the b quark mass tends to infinity (HQET sum rule) [454]. In so doing one has considered the combination of form factors:

$$\mathcal{S}_B(\mathcal{D}_B) = M_Q \text{Im}\ F_1^B(t) \pm \text{Im}\ F_2^B(t)\ , \tag{54.24}$$

corresponding, respectively, to the positive B_Q^+ and negative B_Q^- parity states. Doing the analysis for the Σ_Q, and taking a conservative range of the QCD continuum energy $E_c \approx (1.5 \sim 3)$ GeV, one obtains the mass gap:

$$\delta M_{\Sigma^+} \equiv \Sigma^+ - M_b \approx (1.1 \sim 2.1)\ \text{GeV}\ , \qquad \delta M_{\Sigma^-} \equiv \Sigma^- - M_b \approx (1.8 \sim 2.5)\ \text{GeV}\ , \tag{54.25}$$

https://doi.org/10.1017/9781009290296.068 Published online by Cambridge University Press

respectively for the positive and negative parity states. This result shows that the baryon mass gap is systematically higher than the meson mass one which is about 0.65 GeV. Analogous analysis for the $\Lambda^{\pm}$ baryons shows that, to the approximation we are working, the δM_{Λ^+} sum rule does not present any stability, while one finds that the Σ^- and Λ^- are almost degenerate.

54.4 Hadrons with charm and beauty

From the point of view of quark-gluon interactions, the $B_c(\bar{b}c)$ meson is intermediate between the $\bar{c}c$ and $\bar{b}b$ systems, and it shares with the two heavy-quarkonia common dynamic properties. It is possible to consider the heavy quark and anti-quark as non-relativistic particles, and describe the bound state, adding then the relativistic corrections. On the other hand, B_c, being the lightest hadron with open beauty and charm, decays weakly. Therefore, it provides us with a rather unique possibility of investigating weak decay form factors in a quarkonium system.

The spectroscopy of the $(\bar{c}b)$ mesons and of the (bcq), (ccq) and (bbq) baryons ($q \equiv d$ or s), the decay constant and the (semi)leptonic decay modes of the B_c meson have been extensively discussed in [731] using combined informations from potential models and QSSR. As a result, one obtains [731]:

- **Spectra**
  The spectra of the B_c-like hadrons from potential models are:

$$\begin{aligned} &M_{B_c(\bar{b}c)} = (6.26 \pm 0.02)\ \text{GeV}\ , \qquad M_{B_c^*(\bar{b}c)} = (6.33 \pm 0.02)\ \text{GeV}, \\ &M_{\Lambda(bcu)} = (6.93 \pm 0.05)\ \text{GeV}, \qquad M_{\Omega(bcs)} = (7.00 \pm 0.05)\ \text{GeV}, \\ &M_{\Xi^*(ccu)} = (3.63 \pm 0.05)\ \text{GeV}, \qquad M_{\Xi^*(bbu)} = (10.21 \pm 0.05)\ \text{GeV}, \end{aligned} \tag{54.26}$$

  which are consistent with, but more precise than, the sum-rule results given in [453,454].
- **The decay constant f_{B_c} and other residues**
  The decay constant of the B_c meson is better determined from QSSR than from potential models. The average of the LSR and $q^2 = 0$ moments sum rule gives the result [731]:

$$f_{B_c} \simeq (2.94 \pm 0.12) f_\pi\ , \tag{54.27}$$

  which leads to the leptonic decay rate into $\tau \nu_\tau$ of about $(3.0 \pm 0.4) \times (V_{cb}/0.037)^2 \times 10^{10}\ \text{s}^{-1}$. This result has been obtained for $\tau \simeq (0.04 \sim 0.12)\ \text{GeV}^{-2}$, for $n \simeq 2 \sim 3$, and for $t_c \simeq 50 \sim 67\ \text{GeV}^2$, or equivalently for $E_c \simeq (1.0 \sim 2.1)$ GeV, where $t_c \equiv (M_b + M_c + E_c)^2$. By comparing it with f_B, one can notice that their difference is about M_c as intuitively expected.
  Residues of the different baryons have been also estimated. Their values with the corresponding normalizations can be found in [731,453,454].
- **Semi-leptonic decays of the B_c**
  We have also studied the semi-leptonic decay of the B_c mesons and the q^2-dependence of the form factors, which differs from the usual VDM expectation. We shall come back to this point in the next chapter.

https://doi.org/10.1017/9781009290296.068 Published online by Cambridge University Press

Detection of these particles in the next B-factory machine will then serve as a stringent test of the results from combined potential models and QSSR analysis obtained in [731].

54.5 Mass splittings of heavy quarkonia

The mass splittings of heavy quarkonia have been studied recently using double ratios of exponential sum rules [313] (Section 51.3). One can notice that the sum rule analysis of the mass splittings is insensitive to the change of the continuum threshold t_c, whilst it optimizes at the sum rule scale $\sigma \equiv \tau \simeq 0.9$ (respectively 0.35) GeV^{-2} for the charmonium (respectively bottomium) systems. As emphasized earlier, some observed mass splittings can be used for fixing the QCD parameters α_s and gluon condensate (see the table of Section 51.3). In this section, we give the different predictions obtained once we know these QCD parameters. These predictions are given in the table of Section 51.3. One can notice that there is a fair agreement between the theoretical predictions and the data when available. For a particular interest is the prediction on the $\Upsilon - \eta_b$ mass-splitting in the range $30 \sim 110$ MeV, which can imply the observation of the η_b through the Υ radiative decay. The (non) observation of the η_b through this process is a test of the validity of the resummed Coulombic correction, which differs from the correction obtained from the truncation of the QCD series. In this latter case, the predicted mass splitting is only of the order of 3 to 20 MeV.

54.6 Gluonia spectra

The properties of gluonia from QSSR and some low-energy theorems have been discussed recently in the update work of [688] where complete references to the original works can also be found), which we shall summarize. The most relevant papers for our discussions will be those in [3,734] and [455–457] for the sum rules analysis, those in [686] for the low-energy theorems and vertex sum rules and those in [687,458,450] for the mixings.[1]

We shall consider the lowest dimension gluonic currents that can be built from the gluon fields and which are gauge invariant:

$$\begin{aligned} J_s &= \beta(\alpha_s) G_{\alpha\beta} G^{\alpha\beta}, \\ \theta^g_{\mu\nu} &= -G^\alpha_\mu G_{\nu\alpha} + \frac{1}{4} g_{\mu\nu} G_{\alpha\beta} G^{\alpha\beta} \\ Q(x) &= \left(\frac{\alpha_s}{8\pi}\right) \text{tr}\, G_{\alpha\beta} \tilde{G}^{\alpha\beta}, \end{aligned} \tag{54.28}$$

where the sum over colour is understood. The β function has been defined in Chapter 2, while

$$\tilde{G}_{\mu\nu} = \frac{1}{2} \epsilon_{\mu\nu\alpha\beta} G^{\alpha\beta} \,, \tag{54.29}$$

is the dual of the gluon field strengths. These currents have respectively the quantum numbers of the $J^{PC} = 0^{++}$, 2^{++} and 0^{-+} gluonia,[2] which are familiar in QCD. The former two

[1] Some theoretical reviews and experimental results on the status of gluonia can be found in [688,365,690,735–738].
[2] The pseudotensor 2^{-+} will not be considered here.

https://doi.org/10.1017/9781009290296.068 Published online by Cambridge University Press

enter into the QCD energy-momentum tensor $\theta_{\mu\nu}$, while the later is the $U(1)_A$ axial-anomaly current. We shall also consider the scalar three-gluon local current:

$$J_{3G} = g^3 f_{abc} G^a G^b G^c \ . \tag{54.30}$$

The spectra of the gluonia has been obtained from a QSSR analysis of the generic two-point correlator:

$$\psi_G(q^2) \equiv i \int d^4x \ e^{iqx} \langle 0|\mathcal{T} J_G(x) \left(J_G(0)\right)^\dagger |0\rangle \ , \tag{54.31}$$

built from the previous gluonic currents $J_G(x)$, using the LSR and its ratio $\mathcal{R}(\tau)$. The gluonium contribution to the spectral function enters through its coupling:

$$\langle \ 0|J_G(x)|G \ \rangle = \sqrt{2} f_G M_G^2 \ . \tag{54.32}$$

The results of the analysis are summarized in Table 54.3.

The mass of the three-gluonic bound state as well as its small mixing with the two-gluonic state have been obtained in [457]. The predictions obtained in the table show that the 0^{++} gluonium is the lightest gluonia, which is in good agreement with lattice calculations [739] and QCD-like inequalities [740] results. This agreement is an a posteriori confirmation of the fact that the neglect of the instanton contributions qualitatively discussed in [382] is a good approximation. Moreover, different analysis in the literature also shows that using current models, instanton effects are negligible in the mass calculations.

One should notice that, in addition to the $G(1.5)$ also found from lattice quenched simulation, the low-mass σ_B coupled to the gluonic current is needed in the QSSR analysis for a consistency of the subtracted and unsubtracted sum rules which optimize in different energy regimes. Moreover, a low-mass σ_B is also found in different experiments [690] and is needed in the linear σ model [741,742,743].

54.7 Unmixed scalar gluonia

54.7.1 Masses and decay constants

The mass spectrum of the scalar gluonium has been given in Table 54.3, where, as previously mentioned, a low-mass scalar σ_B below 1 GeV (we have chosen 1 GeV for definiteness in our discussion but a lower value is not also excluded) is needed in addition to the one G of 1.5 GeV, in order to have consistency between the results from the substracted and unsubtracted sum rules.

54.7.2 σ_B and σ'_B couplings to $\pi\pi$

The decays of pure gluonia states have been estimated from the vertex function shown in Fig. 54.1 constrained by a low-energy theorem (LET):

$$V(q^2) \equiv \langle P|\theta^\mu_\mu|P\rangle = q^2 + 2m_P^2 \ , \qquad P \equiv \pi, K, \eta \ , \tag{54.33}$$

https://doi.org/10.1017/9781009290296.068 Published online by Cambridge University Press

Table 54.3. *Gluonia masses and couplings from QSSR*

		Mass (GeV)			
J^{PC}	Name	Estimate	Upper bound	f_G (MeV)	$\sqrt{t_c}$ (GeV)
0^{++}	G	1.5 ± 0.2	2.16 ± 0.22	390 ± 145	$2.0 \sim 2.1$
	σ_B	≤ 1.00 (input)		≥ 1000	
	σ'_B	1.37 (input)		600	
	$3G$	3.1		62	
2^{++}	T	2.0 ± 0.1	2.7 ± 0.4	80 ± 14	2.2
0^{-+}	P	2.05 ± 0.19	2.34 ± 0.42	$8 \sim 17$	2.2
	E/ι	1.44 (input)		$7 : J/\psi \to \gamma\iota$	

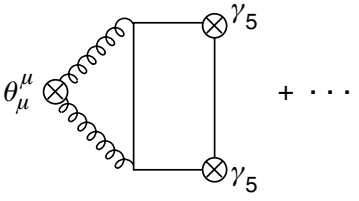

Fig. 54.1. QCD diagram contributing to the scalar gluonium decay into two pseudoscalar Goldstone bosons.

where q is the scalar meson momentum. In the chiral limit, it obeys the dispersion relation:

$$V(q^2) = q^2 \int \frac{dt}{t - q^2 - i\epsilon} \frac{1}{\pi} \mathrm{Im} V(t) \,, \tag{54.34}$$

which gives the first Narison–Veneziano (NV) sum rule [686]:

$$\frac{1}{4} \sum_{S \equiv \sigma_B, \sigma'_B, G} g_{S\pi\pi} \sqrt{2} f_S \simeq 0 \,. \tag{54.35}$$

Using $V'(0) = 1$, and a σ_B meson dominance,[3] it leads to the second NV sum rule:

$$\frac{1}{4} \sum_{S \equiv \sigma_B, \sigma'_B, G} g_{SPP} \frac{\sqrt{2} f_S}{M_S^2} = 1 \,. \tag{54.36}$$

These two sum rules are a generalization of the Goldberger–Treiman relation. It gives the value of the $\sigma_B \pi^+\pi^-$ and $\sigma'_B \pi^+\pi^-$ couplings given in Table 54.4 leading to the unexpected large width of the lowest mass scalar gluonium into pairs of Goldstone bosons.[4]

[3] We could identify the $G(1.5 \sim 1.6)$ with the one observed at GAMS [744] which coupling to $\pi\pi$ is negligible, while for definiteness, we use as input $M_{\sigma'_B} \approx 1.37$ GeV.

[4] Similar results have been obtained in [689].

https://doi.org/10.1017/9781009290296.068 Published online by Cambridge University Press

Table 54.4. *Unmixed scalar gluonia and quarkonia decays*

Name	Mass (GeV)	$\pi\pi$ (GeV)	KK (MeV)	$\eta\eta$ (MeV)	$\eta\eta'$ (MeV)	$(4\pi)_S$ (MeV)	$\gamma\gamma$ (keV)
σ_B	$0.75 \sim 1.0$ (input)	$0.2 \sim 0.8$	$SU(3)$	$SU(3)$			$0.2 \sim 0.3$
σ'_B	1.37 (input)	$0.8 \sim 2.0$	$SU(3)$	$SU(3)$		$43 \sim 316$ (exp)	0.7
G	1.5	≈ 0	≈ 0	$1.1 \sim 2.2$	$5 \sim 10$	$60 \sim 138$	0.5
S_2	1.	0.12	$SU(3)$	$SU(3)$			0.67
S'_2	$1.3 \approx \pi'$	0.3	$SU(3)$	$SU(3)$		4.4	
S_3	1.474 ± 0.044		73 ± 27	15 ± 6		0.4	
S'_3	≈ 1.7		112	$SU(3)$		1.1	

The behaviour of this width versus the mass of the σ_B has been given in [688], where it has been shown that a σ_B of about 600 MeV cannot have a width larger than 150 MeV. The couplings behave analytically as:[5]

$$g_{\sigma_B\pi\pi} \approx \frac{4}{\sqrt{2} f_{\sigma_B}} \frac{1}{\left(1 - M^2_{\sigma_B}/M^2_{\sigma'_B}\right)} , \qquad g_{\sigma'_B\pi\pi} \approx g_{\sigma_B\pi\pi} \left(\frac{f_{\sigma_B}}{f_{\sigma'_B}}\right) . \tag{54.37}$$

The unexpected relatively large width of the σ_B indicates a *large violation of the OZI rule* in the $U(1)$ scalar sector like in the case of the η' decay. As a result from these sum rules, one expects that the scalar gluonium σ_B has an universal coupling (up to $SU(3)$ symmetry breaking terms) to pairs of Goldstone bosons, which is a characteristic feature that should be tested experimentally.

54.7.3 $G(1.5)$ *coupling to* $\eta\eta'$

The coupling of the scalar gluonium to the pairs of $U(1)_A$ mesons ($\eta'\eta'$, $\eta\eta'$) is gouverned by a three-point function made with a glue line shown in Fig. 54.2.

Analogous low-energy theorem [686] gives at $q^2 = 0$:

$$\langle \eta_1 | \theta^\mu_\mu | \eta_1 \rangle = 2 M^2_{\eta_1} , \tag{54.38}$$

where η_1 is the unmixed $U(1)$ singlet state of mass $M_{\eta_1} \simeq 0.76$ GeV. Writing the dispersion relation for the vertex, one obtains the NV sum rule:

$$\frac{1}{4} \sum_{S \equiv \sigma_B, \sigma'_B, G} g_{S\eta_1\eta_1} \sqrt{2} f_S = 2 M^2_{\eta_1} . \tag{54.39}$$

[5] In some LσM approaches, the coupling vanishes in the chiral limit as a reflection of the arbitrariness of the scalar potential term of the effective Lagrangian.

https://doi.org/10.1017/9781009290296.068 Published online by Cambridge University Press

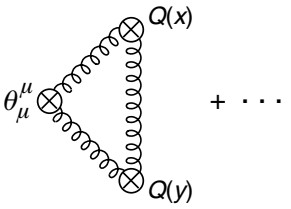

Fig. 54.2. QCD diagram contributing to the scalar gluonium decay into 2 $U(1)_A$ pseudoscalar mesons. $Q(x)$ represents the gluon part of the axial-anomaly.

Assuming a $G(1.5)$ dominance of the vertex, the sum rule leads to:

$$g_{G\eta_1\eta_1} \approx (1.2 \sim 1.7)\ \text{GeV}\ . \tag{54.40}$$

Introducing the 'physical' η' and η through:

$$\eta' \equiv \cos\theta_P \eta_1 - \sin\theta_P \eta_8\ , \qquad \eta \equiv \sin\theta_P \eta_1 + \cos\theta_P \eta_8\ , \tag{54.41}$$

where [16,200] $\theta_P \simeq -(18 \pm 2)^\circ$ is the pseudoscalar mixing angle, one obtains the width given in Table 54.4. The previous scheme is also known to predict (see NV and [746]):

$$r \equiv \frac{\Gamma_{G\eta\eta}}{\Gamma_{G\eta\eta'}} \simeq 0.22\ , \qquad g_{G\eta\eta} \simeq \sin\theta_P g_{G\eta\eta'}\ , \tag{54.42}$$

typical for the $U(1)_A$ anomaly dominance in the decays into η' and η. It can be compared with the GAMS data $r \simeq 0.34 \pm 0.13$, and implies the width $\Gamma_{G\eta\eta}$ in Table 54.4. This result can then suggest that the $G(1.6)$ seen by the GAMS group is a pure gluonium, which is not the case of the particle seen by Crystal Barrel [735] which corresponds to $r \approx 1$. It also shows that the G(1.6) is a relatively narrow state, which may justify the validity of the lattice quenched approximation in the evaluation of its mass.

54.7.4 $\sigma'_B(1.37)$ *and* $G(1.5)$ *couplings to* 4π

Within our scheme, we expect that the 4π are mainly S-waves initiated from the decay of pairs of σ_B. Using:

$$\langle \sigma_B | \theta^\mu_\mu | \sigma_B \rangle = 2M^2_{\sigma_B}\ , \tag{54.43}$$

and writing the dispersion relation for the vertex, one obtains the sum rule:

$$\frac{1}{4} \sum_{i=\sigma_B,\sigma'_B,G} g_{S\sigma_B\sigma_B} \sqrt{2} f_S = 2M^2_{\sigma_B}\ . \tag{54.44}$$

We identify the σ'_B with the observed $f_0(1.37)$, and use its observed width into 4π, which is about (46 ∼ 316) MeV [16] (S-wave part). Neglecting, to a first approximation, the σ_B contribution to the sum rule, we can deduce:

$$g_{G\sigma_B\sigma_B} \approx (2.7 \sim 4.3)\ \text{GeV}\ , \tag{54.45}$$

https://doi.org/10.1017/9781009290296.068 Published online by Cambridge University Press

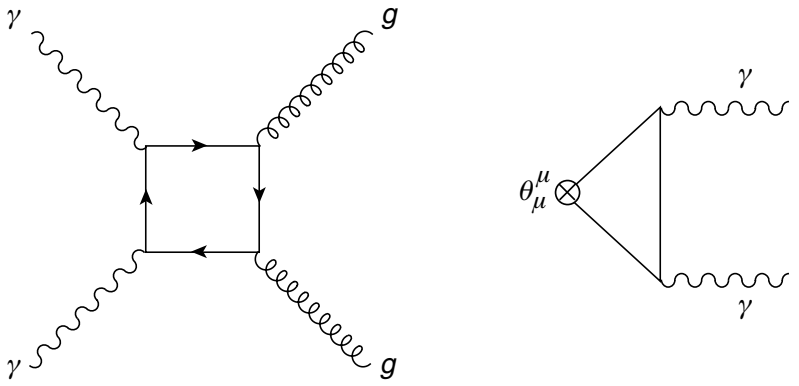

Fig. 54.3. Vertex controlling the gluonium couplings to $J/\psi(\gamma)\gamma$: (a) box diagram; (b) anomaly diagram.

which leads to the width of 60–138 MeV, much larger than the one into $\eta\eta$ and $\eta\eta'$ in Table 54.4. This feature seems to be satisfied by the states seen by GAMS [744] and Crystal Barrel [735]. Our previous approaches show the consistency in interpreting the $G(1.6)$ seen at GAMS as an 'almost' pure gluonium state (ratio of the $\eta\eta'$ versus the $\eta\eta$ widths), while the state seen by the Crystal Barrel, though having a gluon component in its wave function, cannot be a pure gluonium because of its prominent decays into $\eta\eta$ and $\pi^+\pi^-$. We shall see later on that *the Crystal Barrel state can be better explained from a mixing of the GAMS gluonium with the* $S_3(\bar{s}s)$ *and* σ'_B *states.*

54.7.5 σ_B, σ'_B *and* G *couplings to* $\gamma\gamma$

The two-photon widths of the σ_B, σ'_B and G can be obtained by identifying the Euler–Heisenberg effective Lagrangian (see Fig. 54.3) [747]:[6]

$$\mathcal{L}_{\gamma g} = \frac{\alpha\alpha_s Q_q^2}{180 m_q^2}[28F_{\mu\nu}F_{\nu\lambda}G_{\lambda\sigma}G_{\sigma\mu} + 14F_{\mu\nu}G_{\nu\lambda}F_{\lambda\sigma}G_{\sigma\mu} - F_{\mu\nu}G_{\mu\nu}F_{\alpha\beta}G_{\alpha\beta} - F_{\mu\nu}F_{\mu\nu}G_{\alpha\beta}G_{\alpha\beta}] \,, \tag{54.46}$$

with the scalar-$\gamma\gamma$ Lagrangian

$$\mathcal{L}_{S\gamma\gamma} = g_{S\gamma\gamma}\sigma_B(x)F^{(1)}_{\mu\nu}F^{(2)}_{\mu\nu} \,. \tag{54.47}$$

This leads to the sum rule:

$$g_{S\gamma\gamma} \simeq \frac{\alpha}{60}\sqrt{2}f_S M_S^2\left(\frac{\pi}{-\beta_1}\right)\sum_{q\equiv u,d,s}\frac{Q_q^2}{m_q^4} \,, \tag{54.48}$$

[6] $F^{\mu\nu}$ is the photon field strength, Q_q is the quark charge in units of e, $-\beta_1 = 9/2$ for three flavours, and m_q is the 'constituent' quark mass, which we shall take to be $m_u \simeq m_d \simeq M_\rho/2$, $\quad m_s \simeq M_\phi/2$.

https://doi.org/10.1017/9781009290296.068 Published online by Cambridge University Press

from which we deduce the couplings:[7]

$$g_{S\gamma\gamma} \approx (0.4 \sim 0.8)\alpha \text{ GeV}^{-1} , \tag{54.49}$$

($S \equiv \sigma_B,\ \sigma'_B,\ G$) and the widths in Table 54.3, smaller (as expected) than the well-known quarkonia width: $\Gamma(f_2 \to \gamma\gamma) \simeq 2.6$ keV. Alternatively, one can use the trace anomaly: $\langle 0|\theta^\mu_\mu|\gamma_1\gamma_2\rangle$ and the fact that its RHS is $\mathcal{O}(k^2)$, in order to get the sum rule [748,382] ($R \equiv 3\sum Q_i^2$):

$$\langle 0|\frac{1}{4}\beta(\alpha_s)G^2|\gamma_1\gamma_2\rangle \simeq -\langle 0|\frac{\alpha R}{3\pi}F_1^{\mu\nu}F_{2\mu\nu}|\gamma_1\gamma_2\rangle , \tag{54.50}$$

from which one can deduce the couplings:

$$\frac{\sqrt{2}}{4}\sum_{S\equiv\sigma_B,\sigma'_B,G} f_S g_{S\gamma\gamma} \simeq \frac{\alpha R}{3\pi} . \tag{54.51}$$

It is easy to check that the previous values of the couplings also satisfy the trace anomaly sum rule.

54.7.6 $J/\psi \to \gamma S$ radiative decays

As stated in [747], one can estimate the width of this process, using dispersion relation techniques, by saturating the spectral function by the J/ψ plus a continuum. The glue part of the amplitude can be converted into a physical non-perturbative matrix element $\langle 0|\alpha_s G^2|S\rangle$ known through the decay constant f_S estimated from QSSR. By assuming that the continuum is small, one obtains:[8]

$$\Gamma(J/\psi \to \gamma S) \simeq \frac{\alpha^3\pi}{\beta_1^2 656100}\left(\frac{M_{J/\psi}}{M_c}\right)^4\left(\frac{M_\sigma}{M_c}\right)^4\frac{\left(1-M_S^2/M_{J/\psi}^2\right)^3}{\Gamma(J/\psi \to e^+e^-)}f_\sigma^2 . \tag{54.52}$$

This leads to:[9]

$$B(J/\psi \to \gamma S) \times B(S \to \text{ all}) \approx (0.4 \sim 1) \times 10^{-3}. \tag{54.53}$$

for $S \equiv \sigma_B,\ \sigma'_B,\ G$. These branching ratios can be compared with the observed $B(J/\psi \to \gamma f_2) \simeq 1.6 \times 10^{-3}$. The σ_B could already have been produced, but might have been confused with the $\pi\pi$ background. The 'pure gluonium' G production rate is relatively small, contrary to the naïve expectation for a glueball production. In our approach, this is due to the relatively small value of its decay constant, which controls the non-perturbative dynamics. Its observation from this process should wait for the τCF machine. However, we do not exclude the possibility that a state resulting from a quarkonium-gluonium mixing may be produced at higher rates.

[7] Here and in the following, we shall use $M_{\sigma_B} \approx (0.75 \sim 1.0)$ GeV.
[8] We use $M_c \simeq 1.5$ GeV for the charm constituent quark mass and $-\beta_1 = 7/2$ for six flavours.
[9] From the previous results, one can also deduce the corresponding stickiness which is proportional to $\Gamma(J/\psi \to X\gamma)/\Gamma(X \to \gamma\gamma)$ in [736].

https://doi.org/10.1017/9781009290296.068 Published online by Cambridge University Press

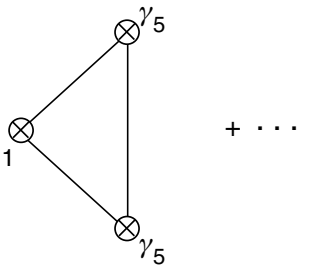

Fig. 54.4. QCD diagram contributing to the scalar $\bar{q}q$ decay into two pseudoscalar mesons Goldstone bosons.

54.7.7 $\phi \to \sigma_B \gamma$ *and* $D_s \to \sigma_B l \nu$ *decays*

From the previous approaches, one also expects to produce the σ_B from ϕ radiative decays [749,688]. Similar analysis can also be done for the $D_s \to \sigma_B l \nu$ semi-leptonic decays [750], where the $\pi\pi$ final state is uniquely produced from a glue rich channel. One should note that due to the large OZI-violation of the $\sigma_B \to \pi\pi$ process, one expects that the $\phi \to \sigma_B \gamma$ and $D_s \to \sigma_B l \nu$ decay rates are sizeable.

54.8 Unmixed scalar quarkonia

The masses of pure $\bar{q}q$ states are given in Table 54.1 and have been obtained using QSSR [3] and [688]. Here S_2 and S_3 denote isoscalar ($I = 0$) scalar states $\bar{u}u + \bar{d}d$ and $\bar{s}s$ and their radial excitations S_2' and S_3'. QSSR predicts a degeneracy between the isovector a_0[10] and isoscalar mass S_2 of about 1 GeV in the absence of mixing, while due to $SU(3)$ breaking the mass of the S_3 is predicted to be in the range of $1.3 \sim 1.4$ GeV. Their widths have been estimated using QSSR for the vertex shown in Fig. 54.4 [751,3] and [688]. These results are compiled in Table 54.4 and indicate that the $\bar{q}q$ *interpretation of the wide* $\sigma(0.6)$ *and* $\kappa(0.9)$ *indicated by some recent data is incompatible with these QSSR results*. The discrepancy with the κ mass is more intriguing, where in this isovector channel, one expects no possible gluon component. The existence of this particle should be further tested from independent and cleaner processes. In the table we quote the updated values from [688], where we have used the fact that the G couplings to $\pi\pi$ and KK are negligible as indicated by the GAMS data [744].

54.9 Mixing schemes for scalar mesons

Previous results for the decay widths of unmixed scalar states can be used using phenomenological mixing schemes in order to explain or to predict the widths of the observed scalar mesons.

[10] One should notice (see Chapter 53), that the a_0 is the particle naturally associated to the divergence of the $SU(2)$ vector current, and which satifies the different chiral symmetry breaking constraints: $m_d - m_u, \ldots$

https://doi.org/10.1017/9781009290296.068 Published online by Cambridge University Press

54.9.1 Nature of the σ and $f_0(0.98)$

Below or around 1 GeV, one can use a two-component mixing as in [687,688] between the gluonium σ_B and quarkonium S_2, and fixes the mixing angle from the predicted $\Gamma(\sigma_B \to \gamma\gamma)$ in Table 54.4 and the observed $\Gamma(f_0 \to \gamma\gamma) \approx 0.3$ keV. In this way one obtains a maximal mixing angle:

$$|\theta_S| \simeq (40 \sim 45)^\circ \,, \tag{54.54}$$

indicating that the f_0 and σ have a large amount of glue and quarks in their wave functions, which is a situation quite similar to the case of the η' in the pseudoscalar channel (mass given by its gluon component but strong coupling to quarkonia).

By recapitulating, our scheme suggests that around 1 GeV, there are two mesons that have $1/2$ gluon and $1/2$ quark in their wave functions resulting from a maximal destructive mixing of a quarkonium (S_2) and gluonium (σ_B) states:

- The $f_0(0.98)$ is narrow, with a width ≤ 134 MeV, and couples strongly to $\bar{K}K$, with the strength $g_{f_0K^+K^-}/g_{f_0\pi^+\pi^-} \simeq 2$, a property seen in $\pi\pi$ and $\gamma\gamma$ scatterings [742] and in $\bar{p}p$ [737] experiments. Its production from ϕ radiative decays is [749]:

$$\Gamma(\phi \to f_0(980)\gamma) \simeq 1.3 \times 10^{-4} \,, \tag{54.55}$$

  in good agreement with recent data from Novosibirsk and Daphne of about 1.1×10^{-4}.
- The σ, with a mass around $(0.75 \sim 1)$ GeV, is large, with a width of about $(400 \sim 900)$ MeV, and has universal couplings to $\pi\pi$ and KK. However, our analysis shows that a σ with lower mass cannot be large.

54.9.2 Nature of the $f_0(1.37)$, $f_0(1.5)$ and $f_J(1.7)$

We use a three-component mixing scheme between the $\sigma'(1.37)$, $S_3(1.47)$ and $G(1.5)$ bare states in order to explain the nature of the above-mentioned three observed states. In order to fix the different angles of the CKM-like 3×3 mixing matrices, we use the following input deduced from the present Crystal Barrel data [752]:

$$\begin{aligned} &\Gamma(f_0(1.50) \to \pi\pi) \simeq (20 \sim 31) \text{ MeV} \qquad \Gamma(f_0(1.50) \to \bar{K}K) \simeq (3.6 \sim 5.6) \text{ MeV} \\ &\Gamma(f_0(1.50) \to \eta\eta) \simeq (2.6 \sim 3.3) \text{ MeV} \qquad \Gamma(f_0(1.50) \to 4\pi^0) \simeq (68 \sim 105) \text{ MeV}, \end{aligned} \tag{54.56}$$

and:

$$\Gamma(f_0(1.50) \to \eta\eta') \simeq 1.3 \text{ MeV} \,. \tag{54.57}$$

We shall also use the widths of the σ' given in the previous table. The resulting values of

https://doi.org/10.1017/9781009290296.068 Published online by Cambridge University Press

the mixing angles read:

$$\begin{pmatrix} f_0(1.37) \\ f_0(1.50) \\ f_0(1.60) \end{pmatrix} \approx \begin{pmatrix} 0.01 \sim 0.22 & -(0.44 \sim 0.7) & 0.89 \sim 0.67 \\ 0.11 \sim 0.16 & 0.89 \sim 0.71 & 0.43 \sim 0.69 \\ -(0.99 \sim 0.96) & -(0.47 \sim 0.52) & 0.14 \sim 0.27 \end{pmatrix} \begin{pmatrix} \sigma'(1.37) \\ S_3(1.47) \\ G(1.5) \end{pmatrix} , \tag{54.58}$$

where the first (respectively second) numbers correspond to the case of large (respectively narrow) σ' widths. From the previous schemes, we deduce the predictions in units of MeV:[11]

$$\Gamma(f_0(1.37) \to \pi\pi) \approx (22 \sim 48) \quad \Gamma(f_0(1.37) \to \eta\eta) \leq 1. \quad \Gamma(f_0(1.37) \to \eta\eta') \leq 2.5 , \tag{54.59}$$

and

$$\Gamma(f_0(1.5) \to \bar{K}K) \approx (3 \sim 12) \quad \Gamma(f_0(1.5) \to \eta\eta) \approx (1 \sim 2) \quad \Gamma(f_0(1.5) \to \eta\eta') \leq 1 , \tag{54.60}$$

despite the crude approximation used, these are in good agreement with the data. These results suggest that the observed $f_0(1.37)$ and $f_0(1.5)$ comes from a maximal mixing between gluonia (σ' and G) and quarkonia S_3. The mixing of the S_3 and G with the quarkonium S_2', which we have neglected compared with the σ', can restore the small discrepancy with the data. One should notice that the state seen by GAMS [744] is more likely to be similar to the unmixed gluonium state G (dominance of the 4π and $\eta\eta'$ decays), as already emphasized in [686], which can be due to some specific features of the central production for the GAMS experiment.[12]

Nature of the $f_J(1.71)$

For the $f_0(1.6)$, we obtain in units of GeV:

$$\begin{aligned} &\Gamma(f_0(1.6) \to \bar{K}K) \approx (0.5 \sim 1.6) \qquad \Gamma(f_0(1.6) \to \pi\pi) \approx (0.9 \sim 2.) \\ &\Gamma(f_0(1.6) \to \eta\eta) \approx (0.04 \sim 0.6) \qquad \Gamma(f_0(1.6) \to \eta\eta') \approx (0.03 \sim 0.07) , \end{aligned} \tag{54.61}$$

and

$$\Gamma(f_0(1.6) \to (4\pi)_S) \approx (0.02 \sim 0.2) , \tag{54.62}$$

which suggests that the $f_0(1.6)$ is very broad and can again be confused with the continuum. Therefore, the $f_J(1.7)$ observed to decay into $\bar{K}K$ with a width of the order $(100 \sim 180)$ MeV, can be essentially composed by the radial excitation $S_3'(1.7 \sim 2.4)$ GeV of the $S_3(\bar{s}s)$, as they have about the same width into $\bar{K}K$ (see Section 6.4). This can also explain the smallness of the $f_J(1.7)$ width into $\pi\pi$ and 4π. Our predictions of the $f_J(1.71)$ width can agree with the result of the OBELIX collaboration [737], while its small decay width into 4π

[11] Recall that we have used as inputs: $\Gamma(f_0(1.37) \to \bar{K}K) \approx 0$, $\Gamma(f_0(1.5) \to \pi\pi) \approx 25$ MeV, while our best prediction for $\Gamma(f_0(1.5) \to (4\pi)_S)$ is about 150 MeV. The present data also favour negative values of the $f_0\eta\eta$, $f_0\eta'\eta$ and f_0KK couplings.

[12] Some alternative scenarios are discussed in [754,755].

https://doi.org/10.1017/9781009290296.068 Published online by Cambridge University Press

is consistent with the best fit of the Crystal Barrel collaboration (see Abele *et al.* in [752]), which is consistent with the fact that the $f_0(1.37)$ likes to decay into 4π. However, the $f_0(1.6)$ and the $f_J(1.71)$ can presumably interfere destructively for giving the dip around $1.5 \sim 1.6$ GeV seen in the $\bar{K}K$ mass distribution from the Crystal Barrel and $\bar{p}p$ annihilations at rest [753,737].

54.10 Mixing and decays of the tensor gluonium

The mass mixing between the tensor gluonium and quarkonium states has been estimated to be small:

$$\theta_T \simeq -10^\circ \,, \tag{54.63}$$

in [450] and [2] using the off-diagonal two-point correlator:

$$\begin{aligned} \psi^{gq}_{\mu\nu\rho\sigma} &\equiv i \int d^4x \, e^{iqx} \langle 0|\mathcal{T}\theta^g_{\mu\nu}(x)\theta^q_{\rho\sigma}(0)^\dagger|0\rangle \\ &= \frac{1}{2}\left(\eta_{\mu\rho}\eta_{\nu\sigma} + \eta_{\mu\sigma}\eta_{\nu\rho} - \frac{2}{3}\eta_{\mu\nu}\eta_{\rho\sigma}\right)\psi_{gq}(q^2) \,, \end{aligned} \tag{54.64}$$

where

$$\theta^q_{\mu\nu}(x) = i\bar{q}(x)(\gamma_\mu \bar{D}_\nu + \gamma_\nu \bar{D}_\mu)q(x) \,. \tag{54.65}$$

Here, $\bar{D}_\mu \equiv \vec{D}_\mu - \overleftarrow{D}_\mu$ is the covariant derivative, and the other quantities have been defined earlier.

The hadronic width of the tensor gluonium has been constrained to be [452,450]:

$$\Gamma(T \to \pi\pi + KK + \eta\eta) \leq (119 \pm 36)\ \text{MeV} \,, \tag{54.66}$$

from the $f_2 \to \pi\pi$ data, and assuming an universal coupling of the T to pairs of Goldstone bosons. A vertex sum rule analogous to the case of the scalar gluonia assumed to be saturated by the f_2 and T leads to:

$$\Gamma(T \to \pi\pi) \leq 70\ \text{MeV} \,. \tag{54.67}$$

These results show that the tensor gluonium cannot be wide. Its width into $\gamma\gamma$ can be related to that of the scalar gluonium G using a non-relativistic relation. In this way one obtains:

$$\Gamma(T \to \gamma\gamma) \simeq \frac{4}{15}\left(\frac{M_T}{M_{0^+}}\right)^3 \Gamma(0^{++} \to \gamma\gamma) \simeq 0.06\ \text{keV}, \tag{54.68}$$

which shows again a small value typical of a gluonium state.

https://doi.org/10.1017/9781009290296.068 Published online by Cambridge University Press

54.11 Mixing and decays of the pseudoscalar gluonium

The mass mixing angle between the pseudoscalar gluonium and quarkonium states has also been estimated from the off-diagonal two-point correlator, with the value [458,3,734]:

$$\theta_P \simeq 12^\circ, \tag{54.69}$$

from which one can deduce:

$$\begin{aligned}\Gamma(P \to \gamma\gamma) &\simeq \tan^2\theta_P \left(\frac{M_P}{M_{\eta'}}\right)^3 \Gamma(\eta' \to \gamma\gamma) \approx 1.3 \text{ keV} \\ \Gamma(P \to \rho\gamma) &\simeq \tan^2\theta_P \left(\frac{k_P}{k_{\eta'}}\right)^3 \Gamma(\eta' \to \rho\gamma) \approx 0.3 \text{ MeV} ,\end{aligned} \tag{54.70}$$

where k_i is the momentum of the particle i. We have used $\Gamma(\eta' \to \gamma\gamma) \simeq 4.3$ keV and $\Gamma(\eta' \to \rho\gamma) \simeq 72$ keV. Measurements of the P widths can test the amount of glue inside the P-meson.

Some other aplications of the sum rules in the pseudoscalar channel will be discussed later on. These concern the estimate of the topological charge and its implications to the proton spin.

54.12 Test of the four-quark nature of the $a_0(980)$

The four-quark nature of the $a_0(980)$ and $f_0(975)$ has been conjectured from the bag model approach [73,757] in order to explain their degeneracy and their large couplings to K^+K^- pairs, where in this scheme, their quark content would be:

$$\begin{aligned}|a_0\rangle &= \frac{1}{\sqrt{2}}\, \bar{s}s(\bar{u}u - \bar{d}d) \\ |f_0\rangle &= \frac{1}{\sqrt{2}}\, \bar{s}s(\bar{u}u + \bar{d}d) .\end{aligned} \tag{54.71}$$

On the other hand, this scheme is unlikely as it does not explain why the usual $\bar{q}q$ scalar states are absent, whilst in addition, it leads to a proliferation of states (many cryptoexotics, ...). Moreover, the relation of this model with the usual chiral and flavour symmetries is not obvious. Within the framework of QSSR, the two-point correlator associated to the colour singlet operators:

$$\mathcal{O}_1^{\pm} = \frac{1}{\sqrt{2}} \sum_{\Gamma=1,\gamma_5} \bar{s}\Gamma s(\bar{u}\Gamma u - \bar{d}\Gamma d) , \tag{54.72}$$

has been firstly studied in [465], where the LSR analysis leads to:

$$M_E \simeq 1 \text{ GeV} , \qquad f_E \simeq 2.5 \text{ MeV} , \tag{54.73}$$

where E corresponds to exotic and f_E is normalized as $f_\pi = 92.4$ MeV. In [756], one has

https://doi.org/10.1017/9781009290296.068 Published online by Cambridge University Press

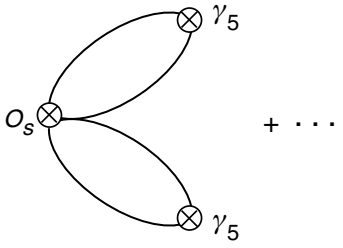

Fig. 54.5. QCD diagram contributing to the a_0 decay into two pseudoscalar bosons in the assumption of a four-quark state.

also introduced the operator:

$$\mathcal{O}_2^{\pm} = \frac{1}{\sqrt{2}} \sum_{\Gamma=1,\gamma_5} \bar{s}\Gamma\lambda_a s(\bar{u}\Gamma u - \bar{d}\Gamma\lambda^a d) \,, \tag{54.74}$$

and studied the more general combination:

$$\mathcal{O}^{\pm} = \mathcal{O}_1^{\pm} + t\mathcal{O}_2^{\pm} \,. \tag{54.75}$$

In this case the decay constant f_E becomes function of t as:

$$f_E \simeq \left(1 + \frac{32}{9}t^2\right)^{1/2} \,. \tag{54.76}$$

A sum rule analysis of the vertex shown in Fig. 54.5 leads to the $a_0 \to \eta\pi, \bar{K}K$ widths [756,3]:

$$\Gamma(a_0 \to \eta\pi) \simeq (52 \sim 88)\ \text{MeV} \left(1 + \frac{32}{9}t^2\right)^{-1} \,, \tag{54.77}$$

and:

$$g_{a_0\bar{K}K} \simeq \sqrt{\frac{3}{2}} g_{a_0\eta\pi} \times \left(1 + \frac{16}{3}t\right) \simeq (5 \sim 8)\ \text{GeV} \,. \tag{54.78}$$

These results indicate that the $a_0\bar{K}K$ coupling can strongly deviate from the $SU(3)$ expectation owing to the extra $(1 + \frac{16}{3}t)$ factor, which is a result expected in this scenario. However, an estimate of the $\gamma\gamma$ width within the same framework, as shown in Fig. 54.6, gives:

$$\Gamma(E \to \gamma\gamma) \approx (2 \sim 5) \times 10^{-4}\ \text{keV} \,, \tag{54.79}$$

which is too small compared with the data for the a_0 of about 0.3 keV. The smallness of this quantity can be better understood if one compares the ratio of the $\gamma\gamma$ couplings obtained

https://doi.org/10.1017/9781009290296.068 Published online by Cambridge University Press

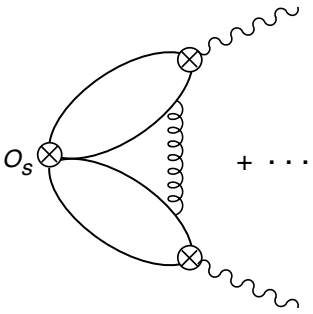

Fig. 54.6. QCD diagram contributing to the a_0 decay into two photons in the assumption of a four-quark state.

from QSSR for the $\bar{q}q$ and four-quark representation of the a_0. At the stability point, one obtains:

$$\frac{g_{E\gamma\gamma}}{g_{a_0\gamma\gamma}} \simeq -\left(\frac{\alpha_s}{\pi}\right)\frac{4t}{27}\frac{\langle\bar{s}s\rangle}{M_E^2 f_E}\frac{f_{a_0}}{(m_d-m_u)}\,, \tag{54.80}$$

where f_{a_0} is proportional to the running quark mass difference $m_d - m_u$. This relation shows the relative suppression of $g_{E\gamma\gamma}$ with respect to the one in the $\bar{q}q$ scheme reproduced correctly by the QSSR method. The coefficients in the previous equation does not support the *rough* estimate [758]:

$$\Gamma(E \to \gamma\gamma)_{(\bar{q}q)^2} \approx 0.24\alpha_s^2\Gamma(a_0 \to \gamma\gamma)_{\bar{q}q}\,, \tag{54.81}$$

which overestimates the width by about two orders of magnitude ($\approx 1/16\pi^2$). This negative result does not support the four-quark nature of the a_0. Further experimental tests are needed for checking this result. We plan to come back to this point in a future work.

54.13 Light hybrids

Hybrid mesons are interesting due to the *exotic* quantum numbers, such that they are not expected to mix with ordinary mesons. A lot of studies have investigated their activities within QSSR [459,460] and the final correct QCD result has been obtained in [461]. In this approach, one can consider the colourless, local and gauge-invariant operators:

$$\mathcal{O}_V^\mu(x) =: \; g\bar{\psi}\lambda_a\gamma_\nu\psi G_a^{\mu\nu} \; : \qquad \mathcal{O}_A^\mu(x) =: \; g\bar{\psi}\lambda_a\gamma_\nu\gamma_5\psi G_a^{\mu\nu} \; : \tag{54.82}$$

corresponding to the vector and axial-vector channels. They are the only lowest dimension operators that can be used to study the quantum numbers of the exotic mesons 1^{-+} an 0^{--}. The corresponding two-point correlator can be decomposed into its transverse spin 1 and

https://doi.org/10.1017/9781009290296.068 Published online by Cambridge University Press

Table 54.5. *Light hybrid masses and couplings from QSSR*

J^{PC}	Name	Mass (GeV)	f_H (MeV)	$\sqrt{t_c}$ (GeV)
1^{-+}	$\tilde{\rho}(\bar{u}gd)$	$1.6 \sim 1.7$	$25 \sim 50$	$M_{\tilde{\rho}} + 0.2$
	$\tilde{\phi}(\bar{s}gs)$	$M_{\tilde{\rho}} + 0.6$		
0^{--}	$\tilde{\eta}(\bar{u}gu + \bar{d}gd)$	3.8	–	4.1

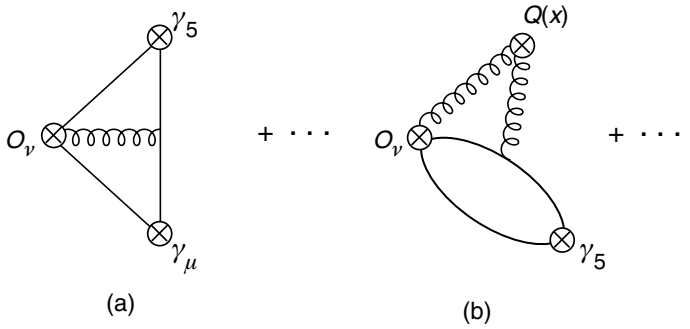

Fig. 54.7. QCD diagram contributing to the $\tilde{\rho}$ decay into (a) $\pi\rho$ and (b) $\pi\eta'$. $Q(x)$ represents the gluon component of the axial-anomaly.

longitudinal spin 0 parts:

$$\Pi^{\mu\nu}_{V/A}(q^2) \equiv i \int d^4x \; e^{iqx} \langle\, 0|\mathcal{T}\mathcal{O}^{\mu}_{V/A}(x) \left(\mathcal{O}^{\nu}_{V/A}(0)\right)^{\dagger} |0\,\rangle$$
$$= -(g^{\mu\nu}q^2 - q^{\mu}q^{\nu})\Pi^{(1)}_{V/A}(q^2) + q^{\mu}q^{\nu}\Pi^{(0)}_{V/A}(q^2)\,. \qquad (54.83)$$

54.13.1 Spectra

The masses of the light hybrids have been obtained in [461,3,462] using LSR within stability criteria and a two-parameter fit of the ratio of moments. The inclusion of the contribution of a new $D = 2$ operator due to tachyonic gluon mass has been considered in [462], but the effect on the mass and coupling predictions is negligible. The updated results [462] are given in Table 54.5.

54.13.2 Decay widths of the $\tilde{\rho}$

The different exclusive decays of the $\tilde{\rho}$ have been studied in [461,3,462] using vertex sum rules shown in Fig. 54.7.

We give the results in Table 54.6. These results show that the $\rho\pi$ is the dominant mode, while $\eta'\pi$ is the most characteristic signal for detecting the $\tilde{\rho}$.

https://doi.org/10.1017/9781009290296.068 Published online by Cambridge University Press

Table 54.6. *Decay modes of the $\tilde{\rho}$ from QSSR*

Decay modes	Width (MeV)	Comments
$\rho\pi$	274	
K^*K	8	
$\gamma\pi$	3	
$\pi\pi$, KK	≈ 0	$\mathcal{O}\left(m_q^2\right)$
$\eta'\pi$	3	$U(1)$ anomaly
$\eta\pi$	$\frac{\Gamma(\tilde{\rho}\to\eta\pi)}{\Gamma(\tilde{\rho}\to\eta'\pi)} \simeq 3.1\tan^2\theta_P$	

Table 54.7. *Heavy hybrid masses from QSSR*

J^{PC}	$\bar{b}gb$	$\bar{c}gc$	$\bar{b}gu$	$\bar{c}gu$
0^{++}	10.9	5.0	6.8	4.0
0^{--}	11.4	5.4	7.7	4.5
1^{+-}	10.6	4.1	–	–
1^{++}	10.9	4.7	6.5	3.4

54.14 Heavy hybrids

The heavy hybrids have been studied within QSSR in [463]. Unfortunately, no independent group has checked their calculations.[13] The results presenting τ stability are given in Table 54.7.

One should notice that the results obtained in [463] have no t_c stability as they increase with t_c. The results in the table correspond to the beginning of τ stability. They correspond to the value of $\sqrt{t_c}$ of about (0.3–0.4) and (0.6–0.7) GeV above the meson masses respectively for the $\bar{c}gc$ and $\bar{b}gb$. For the $\bar{c}gu$ and $\bar{b}gu$, the $\sqrt{t_c}$ values are respectively 0.2 and (0.3–0.4) GeV above the meson masses. One can see from this table that the splitting between two opposite C-parity states is typically (300 $\sim$ 500) MeV, while the spin zero state is much heavier than the spin one, which is similar to the case of light hybrids. These results are in general in agreement with lattice values [759].

54.14.1 Conclusions

There are some progress in the long-term study and experimental search for the exotics. Before some definite conclusions, one still needs improvments of the present data, and some improved unquenched lattice estimates which should complement the QCD spectral sum rule (QSSR) and low-energy theorem (LET) results. Our results cannot absolutely exclude the existence of the 1^{-+} state at 1.4 GeV seen recently in hadronic machines (BNL and

[13] Recently, we have checked some of these results [464].

https://doi.org/10.1017/9781009290296.068 Published online by Cambridge University Press

Crystal Barrel) [760], but at the same time predict the existence of a 1^{--} hybrid almost degenerate with the 1^{-+}, and which could manifest in $e^+e^- \to$ hadrons by mixing with the radial excitations of the ρ mesons. The relatively low value of t_c might also indicate a rich population of (axial-)vector hybrid states in the region aroud 1.8 GeV. In our analysis, the lightest 0^- states are in the range of the charmonium states, such that they could mix with these states as well. A search for heavy hybrid mesons at LHCb or some other B-factories should be useful for testing the theoretical predictions.

https://doi.org/10.1017/9781009290296.068 Published online by Cambridge University Press